Mathiyalagan Kiruthika et al. / Journal of Pharmacy Research 2016,10(10),623-628

Research Article
ISSN: 0974-6943

Available online through
http://jprsolutions.info

Design, Synthesis, Spectral Characterization and Biological Evaluation of Mononuclear Ruthenium(II) Complexes

Mathiyalagan Kiruthika[1] and Periyasamy Dharmalingam[2*]

[1]Department of Chemistry, Arignar Anna Government Arts College, Musiri-621 211,Tamil Nadu, India
[2]Department of Chemistry, Urumu Dhanalakshmi College, Tiruchirappalli, 620 019,Tamil Nadu, India.

Received on:23-07-2016; Revised on: 14-08-2016; Accepted on: 07-09-2016

ABSTRACT

Background: Two new mixed ligand ruthenium(II) complexes of the type $[Ru(bpy)_2(L)](PF_6)_2$ where 2-[4,5-bis(4-dimethylaminophenyl)-1*H*-imidazol-2-yl]-1H-benzimidazole (**1**) and 2-[4,5-bis(4-fluorophenyl)-1*H*-imidazol-2-yl]-1H benzimidazole (**2**) have been synthesized. **Methods:** Both the complexes were characterized by elemental analyses, UV-visible, IR and ESI-MS techniques. Cyclic and differential pulse voltammetry methods have been employed to study the redox behavior of complexes. **Results and Discussion:** Electrophoretic studies showed that the complexes are able to cleave supercoiled plasmid DNA more effectively in the presence of light at the wavelength of 480 nm. Moreover the newly synthesized complexes show better antimicrobial activity compared to that of the ligands. Cytotoxic activity against MCF7 cancer cell lines has been studied using MTT assay. **Conclusion:** Both the complexes exhibit significant biological activities against DNA, microbes and MCF7 cancer cell lines.

Key words: Benzimidazole, ruthenium(II), antimicrobial, MCF7.

1. INTRODUCTION

Though transition metals occupy many key positions in biological processes, metal-based drugs are traditionally undervalued by the pharmaceutical industry, which is dominated by organic chemistry. Nevertheless, a number of coordination compounds have been applied in the therapy of various diseases. Ruthenium is a very good metal to be used in metal complex drugs considering its ability to mimic iron in binding to certain biological molecules. Ruthenium compounds are regarded as promising alternatives to platinum compounds and offer many approaches to innovative metallopharmaceuticals, the compounds are known to be stable and to have predictable structures both in the solid state and in solution: tuning of ligand affinities and accompanied by a steadily increasing knowledge of the biological effects of ruthenium compounds [1, 2]. Many ruthenium compounds are evaluated for clinical applications mostly for cancer treatment. Ru(II) and Ru(III) complexes having the similar ligand exchange rates compared to Pt(II) complex (*cis*-platin, carboplatin, etc.,) which shown to be anticancer agents. Ligand exchange is an important criterion when it comes to clinical applications [3-6]. Very few molecules are able to reach the biological targets without being modified. NAMI-A and KP1019 are the two ruthenium drugs under clinical trials [7]. They have afforded great research interest in anticancer study to overcome the chief limitations of the platinum based drugs [8-10]. Research on mixed ligand metal complexes has been put into practice in order to combine the pharmacological properties of both the ligands and metal thus reduce toxicity simultaneously [11]. In the present work, we have synthesized two new mononuclear mixed ligand ruthenium(II) complexes of type $[Ru(bpy)_2(L)](PF_6)_2$ (where L=2-[4,5-bis(4-dimethylaminophenyl)-1*H*-imidazol-2-yl]-1H-benzimidazole (**1**) and 2-[4,5-bis(4-fluorophenyl)-1*H*-imidazol-2-yl]-1H-benzimidazole (**2**)) have been synthesized and characterized by various physico-chemical techniques. Photocleavage of plasmid DNA, antioxidant, anticancer and antimicrobial activities of the synthesized complexes have been reported.

2. EXPERIMENTAL SECTION

2.1. Materials

Ruthenium chloride trihydrate, ammonium hexafluoro phosphate, 4,4'-difluorobenzil and 4,4'-bis(dimethylamino benzil) were purchased from Sigma-Aldrich. Acetic acid, ammonium acetate, methanol, acetonitrile and ethanol were purchased from SD Fine chemicals. Benzimidazole-2-carboxaldehyde was prepared by following a reported procedure[12].

***Corresponding author.**
Dr.Periyasamy Dharmalingam
Department of Chemistry,
Urumu Dhanalakshmi College,
Tiruchirappalli, 620 019,
Tamil Nadu, India.

2.2. Methods

Absorption spectra were recorded on Shimadzu UV-160A UV-Visible spectrophotometer. Cyclic (CV) and differential pulse voltammetries (DPV) were performed by using CH instrument (USA) model CH-620 B electrochemical analyzer. A conventional three electrode system consisting of platinum disc as a working electrode, platinum wire as an auxiliary electrode and saturated calomel (SCE) as a reference electrode was used for the electrochemical measurements. 0.1 M tetrabutyl ammonium perchlorate (TBAP) was used as the supporting electrolyte for all the experiments. Elemental analyses were performed using Elementar Vario EL III at Sophisticated Test and Instrumentation Centre (STIC), Kerala. Positive ion electronspray ionization mass spectra of the complexes were obtained by using Thermo Finnigan LCQ 6000 advantage max ion trap mass spectrometer. IR spectra were recorded as KBr pellets in the 400 - 4000 cm^{-1} region using a Shimadzu FT–IR 8000 spectrophotometer. All the DNA gel images were taken using UVITEC gel documentation system and fragments were analysed using UVIchem and UVI-band software.

2.3. Synthesis of Ligands

2.3.1. Synthesis of 2-[4,5-bis(4-dimethylaminophenyl)-1H-imidazol-2-yl]-1H-benzimidazole (L1)

4,4'-bis(dimethylamino)benzil (0.2 g, 0.67 mmol), benzimidazole-2-carboxaldehyde (0.103 g, 0.71 mmol) and ammonium acetate (2 g, 25 mmol) were dissolved in 15 mL acetic acid and heated to reflux for 3 h. After cooling, cold water (10 mL) was added to the solution, during which light green precipitate was appeared. It was filtered and recrystallized using ethanol (Yield 0.15 g, 51 %). ESI-MS: m/z 423.5 $(M+1)^+$. Anal. Calc. for $C_{26}H_{26}N_6$: C, 73.91; H, 6.20; N, 19.89. Found: C, 73.88; H, 6.18; N, 19.85. IR, cm^{-1}(KBr pellet) 3369, 3091, 2912, 1641, 1541, 1379, 1253.

2.3.2. Synthesis of 2-[4,5-bis(4-difluorophenyl)-1H-imidazol-2-yl]-1H-benzimidazole (L2)

2-[4,5-bis(4-difluorophenyl)-1*H*-imidazol-2-yl]-1H-benzimidazole was synthesized by using the same procedure described above by reacting benzimidazole-2-carbaldehyde (0.124 g, 0.85 mmol) with 4,4'-difluorobenzil (0.2 g, 0.81 mmol) and ammonium acetate (Yield 0.19 g, 62 %). ESI-MS: m/z 373.4 $(M+1)^+$. Anal. Calc. for $C_{22}H_{14}F_2N_4$: C, 70.96; H, 3.79; N, 15.05. Found: C, 70.92; H, 3.74; N, 15.03. IR, cm^{-1} (KBr pellet) 3436, 3032, 2312, 1668, 1598, 1232.

2.4. Synthesis of Complexes

2.4.1. Synthesis of $[Ru(bpy)_2(L1)](PF_6)_2$ (1).

A mixture of [*cis*-$Ru(bpy)_2Cl_2]\cdot 2H_2O$ (0.2 g, 0.38 mmol) and **L1** (0.14 g, 0.38 mmol) was suspended in an ethanol/water solvent mixture (3/1, v/v). The mixture was refluxed under an inert atmosphere for 4 h while vigorous stirring was maintained. The reaction mixture was cooled to room temperature; the solvent was reduced under vacuum to one-third of its initial volume. A saturated aqueous solution of NH_4PF_6 was added to precipitate $[Ru(bpy)_2(L1)]^{2+}$ as its hexafluorophosphate salt. The product was filtered and washed with water (3 × 10 mL) and then purified by column chromatography on neutral alumina using acetonitrile/toluene (1.5/1, v/v) as an eluent. Yield: 0.2739 g, 67 %. Anal. Calc. for $C_{46}H_{42}F_{12}N_{10}P_2Ru$: C, 49.07; H, 3.76; N, 12.44. Found: C, 49.04; H, 3.74; N, 12.39. ESI-MS: *m/z* 981.83 $(M-PF_6)^+$; IR, cm^{-1}(KBr pellet) 3429, 3097, 1589, 1379, 1247, 840, 765. UV-Visible λ_{max}, nm 277, 323, 508.

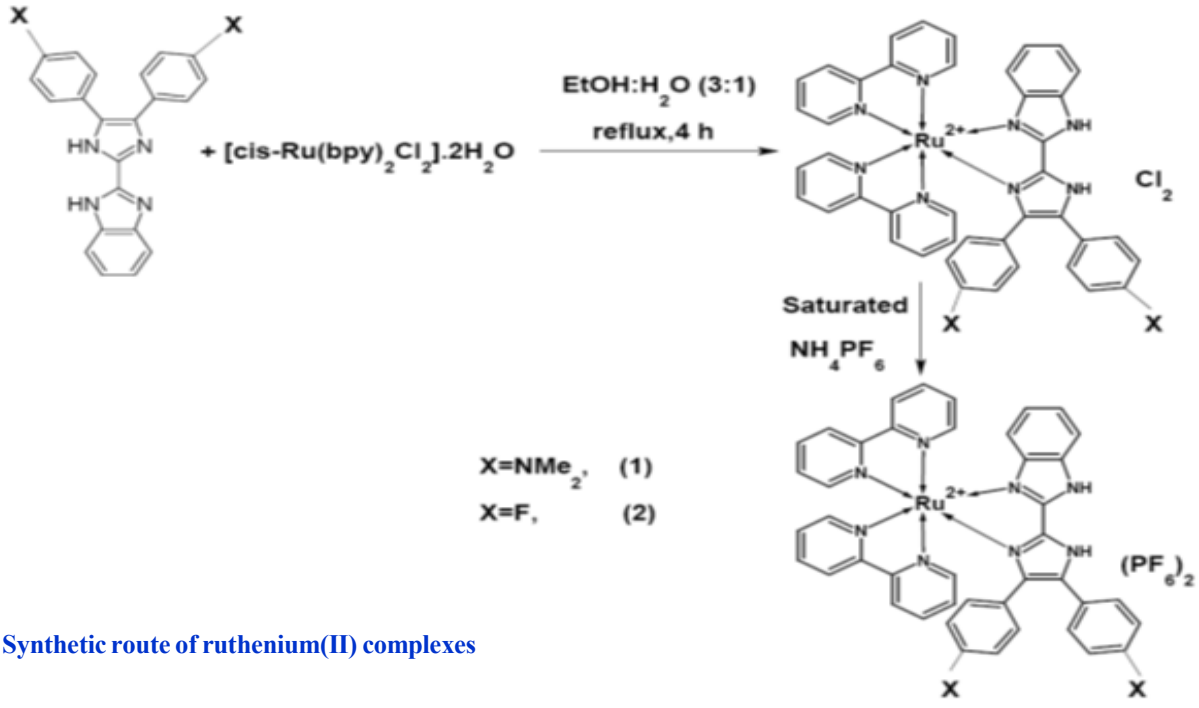

Fig. 1. Synthetic route of ruthenium(II) complexes

2.4.2. Synthesis of $[Ru(bpy)_2(L2)](PF_6)_2$ (2).

The synthesis and purification of compound **2** were similar to those of **1** using $[Ru(bpy)_2Cl_2]\cdot 2H_2O$ (0.2 g, 0.38 mmol) and **L2** (0.12 g, 0.38 mmol). Yield: 0.2299 g, 59 %. Anal. Calc. for $C_{42}H_{30}F_{14}N_8P_2Ru$: C, 46.99; H, 2.81; N, 10.42. Found: C, 46.95; H, 2.78 N, 10.38. ESI-MS: *m/z* 1076.54 $(M+1)^+$; IR, cm^{-1}(KBr pellet) 3394, 3074, 1666, 1598, 1415, 1232, 844, 759. UV-Visible λ_{max}, nm 285, 326, 512.

2.5. DNA Cleavage Activity

Photonuclease activity of the complexes was monitored using gel electrophoresis of plasmid DNA (pUC19). The solutions were prepared for the photolysis experiment containing 3 µL of 100 µg mL^{-1} plasmid DNA in Tris buffer and varying amounts of complexes **1-2** (0–24 µM). Each solution was incubated for 1 hour and then irradiated at 450 nm for various time intervals varying from 10 min to 60 min. The samples were then subjected to electrophoresis in 0.8 % agarose gel (tris-boric acid-EDTA buffer, pH 8.0) at 50 V for 2 h. The gel was stained with 0.5 µg mL^{-1} of ethidium bromide. The stained gel was illuminated under UV lamp and gel documented. In a separate experiment the DNA was incubated with 24 µM of the metal complex and 10 mM of histidine and irradiated at 440 nm. The photolysed solution was subsequently subjected to electrophoresis.

2.6. In vitro Cytotoxicity Assay

3-[4,5-dimethylthiazol-2-yl]2,5-diphenyltetrazolium bromide (MTT) is a yellow water soluble tetrazolium salt. A mitochondrial enzyme in living cells, succinate-dehydrogenase, cleaves the tetrazolium ring, converting the MTT to an insoluble purple formazan. Therefore, the amount of formazan produced is directly proportional to the number of viable cells.

The human breast cancer cell line (MCF 7) was obtained from National Centre for Cell Science (NCCS), Pune and grown in Eagles Minimum Essential Medium (EMEM) containing 10 % fetal bovine serum (FBS). All cells were maintained at 37ºC, 5 % CO_2, 95 % air and 100 % relative humidity. For screening experiments, the cells were seeded into 96-well plates in 100 mL of the respective medium containing 10 % FBS, at a plating density of 10 000 cells/well and incubated at 37 ºC, 5 % CO_2, 95 % air and 100 % relative humidity for 24 h prior to the addition of compounds. The compounds were dissolved in DMSO and diluted in the respective medium containing 1 % FBS. After 24 h, the medium was replaced with the respective medium with 1 % FBS containing the compounds at various concentrations and incubated at 37ºC, 5 % CO_2, 95 % air and 100 % relative humidity for 48 h. Experiments were performed in triplicate and the medium without the compounds served as control. After 48 h, 15 µL of MTT (5 mg mL^{-1}) in phosphate buffered saline (PBS) was added to each well and incubated at 37ºC for 4 h. The medium with MTT was then removed and the formed formazan crystals were dissolved in 100 mL of DMSO and the absorbance measured at 570 nm using a micro plate reader. The % cell inhibition was determined using the following formula, and a graph was plotted between % of cell inhibition and concentration. From this plot, the IC_{50} value was calculated. The % cell inhibition was determined using the following formula.

% Cell Inhibition = 100- Abs (sample)/Abs (control) ×100.

Nonlinear regression graph was plotted between % Cell inhibition and Log concentration and IC_{50} was determined using GraphPad Prism software.

2.7. Antimicrobial Assay

2.7.1. Test Microorganisms:

Two Gram-positive bacteria (*Staphylococcus aureus* and *Bacillus subtilis*), two Gram-negative bacteria (*Escherichia coli* and *Pseudomonas aeruginosa*), and two fungi (*Aspergillus niger* and *Candida albicans*) were used in the present study for evaluation of antimicrobial activity of the synthesized compounds. Medium used for the antimicrobial testing was Muller Hilton agar media and autoclaved at 15 lbs/in2 for 15 minutes.

2.7.2. Antimicrobial Activity:

Agar disc diffusion method was used to study *t*he antimicrobial activity of the newly synthesized compounds. For the evaluation of antimicrobial activity, the size of inoculum was adjusted to approximately 108 colony-forming units (cfu/mL) by suspending the culture in sterile distilled water. Petri dishes containing 20 mL of Muller Hilton agar medium were swabbed with a culture of the respective microbial strains and kept for 15 min for the absorption of culture. Sterile borer is used to create the wells (6mm in diameter), and we added 25, 50, 75 and 100 μL solution of each compound of 25, 50, 75 and 100 µg/mL concentration respectively reconstituted in the DMSO on the pre-inoculated plates. All the plates were incubated at 37ºC for 24 hrs. Antimicrobial activity of all the synthesized compounds was determined by measuring the zone of inhibition around the wells. DMSO was used as a negative control, whereas

Gentamycin was used as positive control. This procedure was performed in three replicate plates for each organism.

3. RESULTS AND DISCUSSION

Analytical data indicated the formation of 1:2 ruthenium complexes with ligands **1** and **2** respectively. The ligands were soluble in ethanol and methanol. The metal complexes were reddish brown coloured, non hygroscopic solids, stable in air, infusible at higher temperature, insoluble in water and many common organic solvents but they are soluble in acetonitrile, DMF and DMSO. The molar conductance values of the complexes **1** and **2** (measured in 10^{-3} M DMF) are 135 and 142 Scm^2 mol^{-1} respectively indicating their non-electrolytic nature. The authenticity of the complexes were established form ESI mass spectral analysis of the complexes **1** and **2** show the base peak at m/z of 981.83 and 1076.54 respectively. The characteristic IR bands of the ligands **L1** and **L2** were assigned at 3369 and 3436 cm^{-1} to –NH stretching frequencies respectively. The stretching frequencies for C-H at 3091 and 3032 cm^{-1} and CH=N at 1589 and 1598 cm^{-1} for ligands **L1** and **L2** respectively**.** The IR spectra of the complexes were compared with that of the free ligands to show the changes during complexation. The IR spectra of the Ru(II) complexes **1** and **2**, showed a broad band around 3493 to 3387 cm^{-1} due to the amine and the lattice water peaks. The γ(C=N) stretching vibration, in the free ligand at 1589 and 1598 cm^{-1} for **L1** and **L2** has been shifted to 1587 and 1595 cm^{-1} proving that the azomethine nitrogen is involved in co-ordination. The band at 3091 and 3032 cm^{-1} for **L1** and **L2** which are responsible for γ(C-H) stretching vibration have been shifted to 3081 and 3074 cm^{-1} respectively for complexes **1** and **2** during complex formation. Spectroscopic properties of the complexes were studied in acetonitrile. The electronic spectra of the ligands **L1** and **L2** show bands at 274-277 and 319-328 nm. The first band corresponds to the $\pi \rightarrow \pi^*$ transition and band at 319-328 nm corresponds to $n \rightarrow \pi^*$ transition associated with the >C=N functional groups of the ligands. The absorption spectra of these complexes are typical of the ruthenium polypyridyl complexes with intense UV bands assignable to ligand-centered transitions at 277, 323 nm for complex **1** and 326, 285 nm for complex **2**. Metal to ligand charge transfer (MLCT) transition is observed as a slightly broad band in the visible region at 508 and 512 nm for complex **1** and **2** respectively. The redox behaviour of ruthenium complexes was studied with the help of cyclic voltammetry and the redox properties are presented in Table 1. The cyclic voltammogram of complex **1**, $[Ru(bpy)_2(L1)](PF_6)_2$ measured in acetonitrile solution at 100 mVs^{-1} scan rate features the oxidation of Ru^{II} to Ru^{III} at the anodic peak potential of +0.9314 V. Reduction of Ru^{III} occurs at +0.8599 V upon scan reversal. The separation between the anodic and cathodic peak potentials, ΔEp is at 71 mV. Thus the cyclic voltammetric responses give evidence for the presence of Ru^{II}/Ru^{III} redox couple involving in quasi-reversible one electron redox process. The $E_{1/2}$ value calculated is +0.8957 V. Complex **2**, $[Ru(bpy)_2(L2)](PF_6)_2$ registers cathodic peak potential at +0.8601 V and anodic peak potential at +0.9395 V at the scan rate of 100 mVs^{-1}. The separation between the peak potentials is 79 mV. These values indicate the presence of Ru^{II}/Ru^{III} redox couple and the redox reaction is quasi-reversible in nature. The $E_{1/2}$ value appearing at +0.8998 V points to the fact that Ru^{II} in the complex species may not undergo reduction easily. It can be seen from the Table 1 that the Ru^{II}/Ru^{III} redox potential is influenced by the substituents on the phenyl group. Fluoro group is more electron withdrawing compared to dimethylamino group. Due to this reason Ru^{II}/Ru^{III} redox potential of fluoro substituted complex **2** is more positive compared to dimethylamino substituted complex **1**.

Table 1. Electrochemical parameters for the ruthenium(II) complexes 1 and 2 at the scan rate of 100 mvs^{-1}

Compound	E_{pc} V	E_{pa} V	ΔE_p V	$E_{1/2}$ V
$[Ru(bpy)_2(L1)](PF_6)_2$ (**1**)	0.8599	0.9314	0.071	0.8957
$[Ru(bpy)_2(L2)](PF_6)_2$ (**2**)	0.8601	0.9395	0.079	0.8998
Compound	**I_{pa} ($x10^{-5}$A)**	**I_{pc} ($x10^{-5}$A)**	**I_{pa}/I_{pc}**	
$[Ru(bpy)_2(L1)](PF_6)_2$ (**1**)	3.0251	1.1044	2.73	
$[Ru(bpy)_2(L2)](PF_6)_2$ (**2**)	4.5617	1.6762	2.72	

3.1. BIOLOGICAL STUDIES

3.1.1. DNA cleavage activity

The interaction of plasmid pUC19 DNA with newly synthesized Ru(II) complexes was studied using agarose gel electrophoresis method. The gel picture showing the cleavage of plasmid pUC19 DNA is depicted in Fig. 2. In the present study, the Ethidium bromide (EtBr) stained banding pattern of plasmid pUC19 DNA was tested with newly synthesized ruthenium complexes. No cleavage activity has been obtained in the absence of light. Apparently the complexes show efficient cleavage activity upon irradiating them in the light at the wave length of 480 nm.

The control experiments did not show any apparent cleavage of DNA (lane 1). It was observed that both the complexes were able to cleave DNA at the concentration of 24 µM (lanes 2 and 3). DNA cleavage mechanisms by the present complexes were investigated in the presence of singlet oxygen quencher (Histidine) and hydroxyl radical scavenger (DMSO) under our experimental conditions. Both histidine and DMSO had no effect on the cleavage reaction (lanes 4-7). This suggests that the singlet oxygen and hydroxyl radicals are

not involved in the cleavage reaction. This result clearly indicates that DNA damage occurs through guanine base oxidation of DNA by excited state of ruthenium complexes.

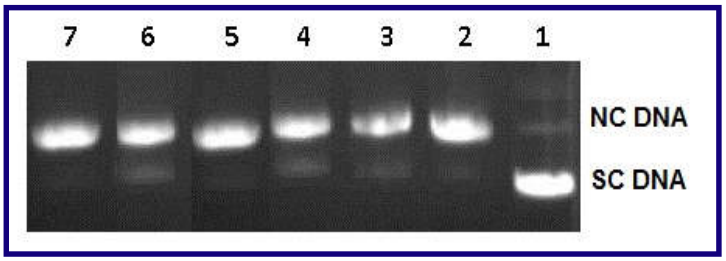

Fig. 2. Cleavage of supercoiled pUC19DNA by the complexes 1 and 2 when incubated for 1 h and followed by irradiation at 480 nm for 30 min (Lane 1-7). Lane 1: DNA alone; Lane 2: DNA+24 µM complex 1; Lane 3: DNA+24 µM complex 2; Lane 4: DNA+24 µM complex 1+Histidine; Lane 5: DNA+24 µM complex 1+DMSO; Lane 6: DNA+24 µM complex 2 + Histidine; Lane 7: DNA +24 µM complex 2 +DMSO.

3.1.2. Antimicrobial studies

In-vitro microbial activity against certain bacterial and fungal species was screened for the free ligands and the ruthenium complexes using disc diffusion method. The antimicrobial activities of the newly synthesized ligands and complexes were tested against the pathogens *viz., Staphylococcus aureus, Bacillus subtilis, Pseudomonas aeroginosa, Escherchia coli, Aspergillus niger* and *Candida albicans.* The results illustrated in (Table 2 and 3) revealed that the tested compounds had a good antibacterial activity than the standard antibiotics. However, in most of the cases they possessed 50 % of the activity of the standards. Compound **1** showed a greater activity than **2** on almost all the pathogens. Compound **1** showed pronounced activity against *Candida albicans, Escherchia coli* and *Aspergillus niger.* Compound **2** showed good activity against *Aspergillus niger* and a moderate activity against all the other organisms under study. The standards used for the antibacterial and antifungal activity were *Gentamycin* and *Clotrimazole* respectively. The anti-microbial activity for the complexes has been found to be greater than the free ligands. This can be attributed to the Tweedy's chelation theory according to which chelation reduces the polarity of the metal atom mainly because of the potential sharing of its positive charge with the donor group and possible π-electron delocalization over the whole ring. This increases the lipophilic character of the metal chelate, favouring its permeation through the lipid layers of the bacterial membranes. Furthermore, the mode of action of the compounds may involve hydrogen bonding *via.,* the >C=N group with active centers of cell constituents resulting in the interference with normal cell process. The activities of the complexes have been compared with the activity of the standard bacteriocide (Gentamycin) and fungicide (Clotrimazole) and it has been found that the complexes show better activity.

Table 2. Antibacterial activity of ligands and their ruthenium(II) complexes

S. No	Test Drug	Zone of Inhibition (mm)															
		S. aureus				*B.Subtilis*				*E. coli*				*P.aeruginosa*			
		25 µg/mL	50 µg/mL	75 µg/mL	100 µg/mL	25 µg/mL	50 µg/mL	75 µg/mL	100 µg/mL	25 µg/mL	50 µg/mL	75 µg/mL	100 µg/mL	25 µg/mL	50 µg/mL	75 µg/mL	100 µg/mL
1	L1	10	11	13	14	10	11	13	16	9	11	13	15	9	13	15	18
2	L2	10	12	14	16	10	11	13	15	10	12	15	18	10	12	15	18
3	1	22	26	32	35	11	14	18	22	18	21	25	32	15	18	20	22
4	2	17	21	25	27	13	15	18	21	15	20	22	25	14	16	18	20
5	Gentamycin	-	-	-	17	-	-	-	18	-	-	-	18	-	-	-	18
	Standard																

Note: Zone size less than 15 mm – Least active; 16 – 20 mm– moderatively active; Above 20 mm – highly active

Table 3. Antifungal activity of ligands and their ruthenium(II) complexes

S. No	Test Drug	Zone of Inhibition (mm)							
		A. niger				*C. albicans*			
		25 µg/mL	50 µg/mL	75 µg/mL	100 µg/mL	25 µg/mL	50 µg/mL	75 µg/mL	100 µg/mL
1	L1	9	10	12	14	13	15	17	20
2	L2	9	10	11	13	10	13	15	18
3	1	16	18	20	25	14	16	20	22
4	2	16	20	24	28	13	16	21	25
5	Clotrimazole	-	-		35	-	-	-	20
	Standard								

Note: Zone size less than 15 mm – Least active; 16 – 20 mm– moderatively active; Above 20 mm – highly active

3.1.2. In-vitro anticancer activity

Of the various human diseases, cancer is the most intractable disease for which no practical and generally effective drugs or methods of control are available. Therefore, the identification of novel, potent, selective, and less toxic anticancer agents remains one of the most pressing problems. Cancer is a complex disease that is a normally associated with a wide range of escalating effects both at the molecular and cellular levels. The compounds **1** and **2** synthesized were evaluated for their cytotoxicity against human breast cancer cell line MCF-7 by means of MTT assay that measured mitochondrial dehydrogenase activity as an indication of cell viability. The results were analysed by means of cell viability curves and expressed in IC_{50} values in the studied concentration range of 0.25 to 100 µM. The activity of the compounds that corresponds to the inhibition of cancer cell growth at a maximum level is shown in Fig.3.

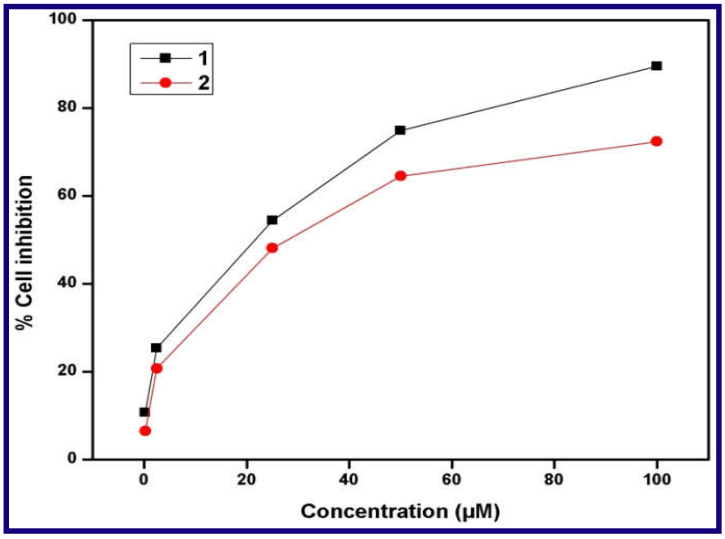

Fig. 3. Percentage growth inhibition of MCF-7 cell line as a function of concentration of the compounds 1 and 2

The results of MTT assay revealed that the compound **2** possessed higher cytotoxic effect than **1**. The presence of fluoro substituent in **2** has enhanced the cytoxicity compared to **1.** The data obtained for our compounds showed cytotoxicity with short incubation period (48 h) and hence the data are highly significant.

4. CONCLUSIONS

Mixed ligand ruthenium(II) mononuclear complexes have been synthesized and characterized using physico-chemical methods. The electrochemical properties of the complexes have been found to be quasi-reversible. The complexes are able to cleave DNA in the presence of light radiation. Antimicrobial activity of the complexes has been found to be greater than that of the synthesized ligands. And also the complexes show better anticancer activity against MCF7 breast cancer cell lines.

ACKNOWLEDGEMENT

MK thanks UGC, New Delhi, India, for providing financial support in the form of MRP.

REFERENCES

1. Song H, Kaiser JT, Barton JK, Crystal structure of Δ-$[Ru(bpy)_2dppz]^{2+}$ bound to mismatched DNA reveals side-by-side metalloinsertion and intercalation, Nat Chem 4, 2012, 615-20.
2. Gorman BA, Francis PS, Barnett NW, Tris(2,2'-bipyridyl)ruthenium(II) chemiluminescence, Analyst, 131, 2006, 616-39.
3. Wong E, Giandomenico CM, Current status of platinum-based antitumor drugs, Chem Rev, 99, 1999, 2451-66.
4. Farrell N, Platinum-based drugs in cancer therapy, Totowa (NJ): Humana Press, 2000.
5. Wheate NJ, Collins JG, Multi-nuclear platinum complexes as anti-cancer drugs, Coord Chem Rev, 241, 2003, 133-45.
6. Galanski M, Arion VB, Jakupec MA, Keppler BK, Recent developments in the field of tumor-inhibiting metal complexes, Curr Pharm Des, 9, 2003, 2078-89.
7. Sava G, Gagliardi R, Bergamo A, Alessio E, Mestroni G, Treatment of metastases of solid mouse tumours by NAMI-A: comparison with cisplatin, cyclophosphamide and dacarbazine, Anticancer Res, 19, 1979, 969-72.
8. Li L, Cao W, Zheng W, Fan C, Chen T, Ruthenium complexes containing 2,6-bis(benzimidazolyl)pyridine derivatives induce cancer cell apoptosis by triggering DNA damage-mediated p53 phosphorylation, Dalton Trans, 41, 2012, 12766-72.
9. Sánchez-González PD, López-Hernández FJ, López-Novoa JM, Morales AI, An integrative view of the pathophysiological events leading to cisplatin nephrotoxicity, Crit Rev Toxicol, 41, 2011,803-21.
10. Bhatarai B, Gramatica P, Per-and polyfluoro toxicity (LC_{50} Inhalation) study in rat and mouse using QSAR modeling, Chem Res Toxicol, 23, 2010, 528-39.
11. Li F, Mulyana Y, Feterl M, Warner JM, Collins JG, Keene FR, The antimicrobial activity of inert oligonuclear polypyridylruthenium(II) complexes against pathogenic bacteria, including MRSA, Dalton Trans, 40, 2011, 5032-8.
12. Sathyaraj G, Kiruthika M, Weyhermuller T, Nair BU, Ruthenium(II) [3 + 2 + 1] mixed ligand complexes: substituent effect on photolability, photooxidation of bases, photocytotoxicity and photonuclease activity, Dalton Trans, 41, 2012, 8460-8471.

Source of support: UGC, New Delhi, India, **Conflict of interest: None Declared**